Generic and real-time detection of specular reflections in images

Alexandre Morgand[1] and Mohamed Tamaazousti[1]
[1]*Vision & Content Engineering Laboratory, CEA LIST, Gif-sur-Yvette, France*
{*alexandre.morgand, mohamed.tamaazousti*}*@cea.fr*

Keywords: Real-time, Generic, Specular reflection detection, HSV, Saturation, Value, Contrast, Gradient, Gravity center

Abstract: In this paper, we propose a generic and efficient method for real-time specular reflections detection in images. The method relies on a new thresholding technique applied in the Hue-Saturation-Value (HSV) color space. A detailed experimental study was conducted in this color space to highlight specular reflections' properties. Current state-of-the-art methods have difficulties with lighting jumps by being too specific or computationally expensive for real-time applications. Our method addresses this problem using the following three steps: an adaptation of the contrast of the image to handle lighting jumps, an automatic thresholding to isolate specular reflections and a post-processing step to further reduce the number of false detections. This method has been compared with the state-of-the-art according to our two proposed experimental protocols based on contours and gravity center and offers fast and accurate results without *a priori* on the image in real-time.

1 INTRODUCTION

Depending on the desired application, specular reflections present advantages and drawbacks in the computer vision community and are subject of many years of studies ((Shafer, 1985), (Blake and Brelstaff, 1988), (Saint-Pierre et al., 2011)). Indeed, they give accurate information for light sources modeling by being defined as a trace of the light sources. This property allows to understand and model light behavior in a scene. For image processing, operations such as segmentation, detection or matching, the presence of specular reflections can disrupt results.

Dealing with specularities in computer vision presents numerous and diversified applications. For example, in color segmentation such as in (Deng et al., 1999), specular reflections are often considered as disturbing and create discontinuities in the segmentation process. In the medical field, they produce false positives in abnormality detection applications. Therefore, they are removed by inpainting methods ((Lee et al., 2010), (Oh et al., 2007), (Saint-Pierre et al., 2011) and (Stehle, 2006)). Conversely, important scene information could be extracted from them to analyse a surface shape (Blake and Brelstaff, 1988) and compute 3D position of the light source, identify surface smoothness, granularity or aspect (mirror-like or glossy surfaces) and could be used for camera localization (Lagger et al., 2008). Moreover, specular reflections are essential elements for a realistic rendering in image synthesis ((Karsch et al., 2011) and (Sillion and Puech, 1989)), or Augmented Reality applications (Jachnik et al., 2012). Lighting effects such as shadow casting or global illumination on a virtual object improve drastically the rendering quality.

Nevertheless, detection of specular reflections is a challenging task: handling reliably large range of brightness (high contrasts, dark or bright images) and different light sources of various intensities are complex issues. Therefore, state-of-the-art methods are very specific and mostly limited to their chosen field of applications. However, specularities present many features common in all of these field of applications but finding these features in an image could represent a high computational cost. Our method targets a large range of field of application without *a priori* on the lighting conditions running in real-time by using simple but effective properties of specular reflections.

In this paper we present the related methods used for specularity reflections detection by highlighting the different applications targeted and results along their limitations. These methods are divided in two approaches: (offline 2.1 and online 2.2 detection). In the section 3, our proposed method without *a priori* is described by highlighting the reliability, efficiency and genericity of the method in real-time. The pre-processing section 3.2 details our contrast equalization algorithm to handle oversaturated images. In 3.3, our automatic thresholding method is presented to handle different lighting conditions increasing the

genericity of our method. In the post-processing 3.4 section, by using the gradient aspect of specularities, misdetected specularities are removed. Our results are presented and compared in 4 with the method of (Arnold et al., 2010) to point out efficiency and genericity of our method.

(a) Specular reflections (b) Complex case of specular reflections

Figure 1: (a) Example of specular reflections on a plane surface: five specularities can be seen and stand out to the eye as saturated elements. (b) Example of a complex case of specular reflections: specularities appeared on the ring in the bottom-middle and on the table in the middle.

2 RELATED WORKS

Specular reflections detection is usually divided in three processes: pre-treatment to handle noise and different lighting conditions, thresholding to isolate specularities by using a predefined or automatically computed thresholds and a post-treatment process to remove misdetected specularities or find missing ones. These steps were used in Table.1 along other criteria such as the color space used and input type (video or image) to give an accurate overview of the state-of-method methods as well as our approach.

2.1 Offline approaches

(Stehle, 2006) used a thresholding on the YUV color space where Y represents the brightness and U, V are the chrominance channels. By thresholding the Y channel at the last peak in the Y histogram, specularities are isolated. According to (Stehle, 2006) a small peak corresponding to specular reflections' pixels can be found on the right hand side of the histogram. This method is used in endoscopic imaging where the context of work is darker and the dynamic range of images is generally well distributed. Nevertheless, with images specular-free, using this method could produce misdetections such as white objects and images with specularities does not have necessarily a peak at the end of the histogram.

(Oh et al., 2007) consider specular reflections as a reflection from a smooth shiny surface visually represented as absolutely bright regions. These highlights appeared as at least one saturated color which is visually *white* as shown in Fig.1(a). In their method, the image is transferred into the Hue-Value-Saturation color space because it is less sensitive to the noise. Firstly, these *Absolute Bright regions* are isolated by two thresholds on the Value and Saturation channels and Hue is left aside because the hue of a saturated color is not defined.

Secondly, a color quantization and a spatial segmentation is applied cutting the image into k regions. By using the same thresholding method on the k regions, they obtained two areas called *Absolute Bright Areas* and *Relative Bright Areas*.

The merging of *Absolute Bright Areas* and *Relative Bright Areas* gives reliable results but using a segmentation method has a algorithmic complexity of $O(n^2)$. Moreover, with *Relative Bright Areas*, it is possible to detect white surfaces which are not specular reflections.

Machine learning, dimensionality reduction and optimization algorithms could be used to isolate specular reflections. (Park and Kak, 2003) proposed a *Truncated Least Squares* approach to map color distribution between images of an object under different illuminations to detect specular highlights. (Lee et al., 2010) uses a perceptron neural networks to classify specular regions. These methods offer good results but are well known for their computationally cost.

(Torres et al., 2003) and (Ortiz and Torres, 2006) highlighted the importance of using a specific color space such as HSV because the perception system of the human brain uses basic attributes of color such as intensity, hue and saturation. They work in a bi-dimensional histogram called the MS diagram and use thresholding to isolate specularities. An histogram equalization is used to keep the threshold constant. These methods give accurate and fast results but using a histogram equalization could lead to false detections because operations which highlight outliers such as the *top-hat contrast operator* enhance specularities but white surfaces and noise as well. Even if artifacts can often be removed by using morphological transformations such as dilation, these morphological operations have an algorithmic complexity of $O(n^2)$ which can be problematic when dealing with video streams for an online detection. Moreover, a specular reflections can appear fragmented into smaller specularities and could be removed by morphological operations like erosion.

2.2 Online approaches

Many fields require real-time method for specularity detection such as medical (Arnold et al., 2010) or Augmented Reality ones (Jachnik et al., 2012).

(Arnold et al., 2010) give another approach of specularities detection problem using threshold in the RGB color space and a gray-scale image. In the RGB color space, *saturated blue, red or green* are considered as specular reflections. Instead of setting a constant global threshold like in (Oh et al., 2007), (Arnold et al., 2010) use an *adaptive threshold* computed from the green and blue color channels to isolate the specular reflections. Another step of thresholding is used to find missed outliers using a modified median filter and a more tolerant thresholding.

The post-processing stage computes the contours of the specular reflections and removes areas of substantial size because they are more likely to be bright regions and not specular reflections.

For endoscopic imaging, this method is reliable and relatively fast but is lacking genericity and is very sensitive to white surfaces. Moreover, endoscopic systems allow to have an accurate control on the light source and provide an efficient automatic exposure correction which ensure to avoid over/underexposure cases.

3 PROPOSED METHOD

3.1 Overview

Our method is aimed to avoid limitations in the specularities detection. The goal is to handle multiple lighting sources with different intensities in real-time. We do not assume the histogram of the image well equalized. Conversely, every lighting issue occurring in a video stream has to be taken into account (as seen in Fig.2(a) and Fig.2(b)). No *a priori* on the specularity size is assumed, bright regions (called Lambertian surfaces [1]) has to be left aside but specularities due to the sun, which has generally a significant size (see Fig.2(d)) must be detected. Our detector must be fast enough to be used in real-time applications.

The color space choice is justified by the behavior of the human eye. A human eye is more sensitive to the blue, green and red zones in order to compute the visual aspect of an object. However, in the perception process of the human brain, the amount of red, green, and blue in objects is not precisely estimated. Instead, basic attributes of color such as intensity, hue, and saturation are used (Ortiz and Torres, 2006). Thus, we decided to work in the HSV color space because specularities stand out naturally in it (see Fig.3) and two criteria can be used in the HSV color space (see Fig.3(b)) as opposed to one criterion in the RGB color space (see Fig.3(a)). Indeed, in the HSV color space, specularities are characterized by a low saturation and a high value whereas in the RGB color space, they are represented by white surfaces.

[1] see (Lambert and DiLaura, 2001) for more details

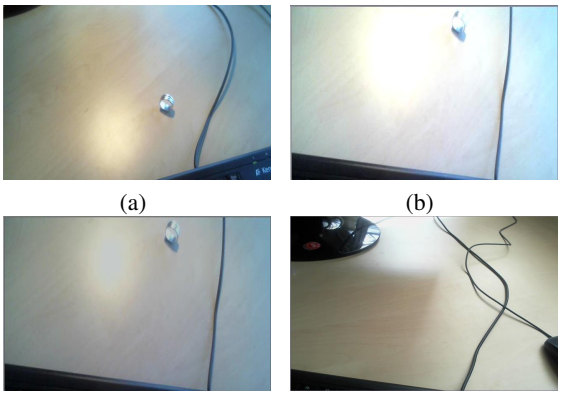

(a) (b) (c) (d)

Figure 2: Different cases of specularities: (a) shows the normal case with good dynamic range. The specularity can be seen on the ring, (b) presents the oversaturated case which is in unusable state, (c) shows the image (b) after our contrast equalization (d), shows a specularity created by the sun which should be detected.

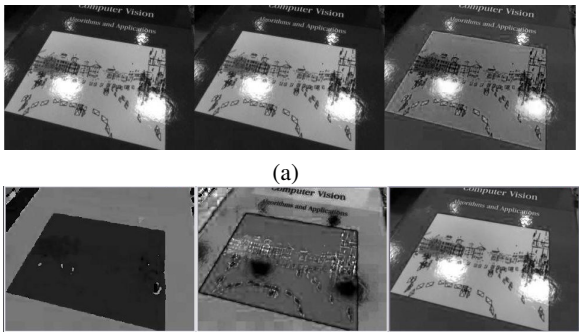

(a) (b)

Figure 3: Specularities follow one criterion in the RGB color space, in the form of white spots. Two criteria can be used in the HSV color space, finding black spots in the Saturation channel and white spots in the Value channel. In (a) RGB channels decomposition, specularities appeared in the three channels Red (left), Green (middle) and Red (left) as bright and white spots. In (b), HSV channels decomposition, specularities can not be seen in the Hue channel (on the left) but clearly in the Saturation channel (in the middle) as black spots and in the Value channel (on the right) as bright and white spots.

Table 1: Main state-of-the-art method classification and positioning of our method.

Properties / Methods	Color space	Threshold	Pre-treatment	Post-treatment	Video/ Image
(Ortiz and Torres, 2006)	MS	constant	Histogram equalization	Morphological operations	Image
(Stehle, 2006)	YUV	automatic	None	Morphological operations	Image
(Oh et al., 2007)	HSV	constant	Top hat operator	Segmentation and Morphological operations	Image
(Arnold et al., 2010)	RGB + gray scale	automatic	None	Morphological operations	Video
Our method	**HSV**	**automatic**	**Contrast**	**Gradient**	**Video**

3.2 Pre-processing

Saturated images often result (Fig.2(b)) in misdetection and are in unusable state. Therefore, a contrast equalization is applied to this image by measuring the brightness of the image as defined in Eq.(1). If this value is above a certain threshold T_b (brightness threshold), the image is considered as saturated and the contrast is lower (see Algorithm.1). The result of this algorithm can be seen in Fig.2(c).

$$\text{Brightness} = \frac{\sqrt{0.241*C_R^2+0.691*C_G^2+0.068*C_B^2}}{Width*Height} \quad (1)$$

The brightness is a relevant factor to use for automatic thresholding because an increase in the brightness causes an increase in the Value channel.

Algorithm 1 Contrast equalization algorithm. Average brightness corresponds to a value of 80. We noticed that saturated images in our training database had a brightness above 125. Due to the uncertain nature of oversaturated images, T_b is set to 125 in order to limit false detections to the maximum possible.

```
contrast = 1;
if Brightness ≤ T_b then
    while Brightness ≤ T_b do
        Contrast ← Contrast − 0.01;
        Image_pixels * Contrast;
        Compute(Brightness);
    end while
end if
```

3.3 Thresholding process

To deal with different lighting conditions and contrasts, we can apply an histogram equalization on the Value channel. However, as (Ortiz and Torres, 2006) pointed out that contrast enhancement is not the best solution as it can sometimes cause oversaturation and an excessive increase in intensity resulting in a false detection of specularities. Therefore, instead of having constant thresholds (as in (Oh et al., 2007) and (Ortiz and Torres, 2005)), our Value threshold is estimated dynamically by using brightness and information in the Value channel histogram. On a training database of 50 samples of greatly varied images with different sizes, contrast, lighting context and lighting intensities, a relation of proportionality with k was found experimentally between the brightness (see Eq.(2)) and T_v which is our threshold Value. For each image, an optimal T_v was manually estimated (see Fig.4).

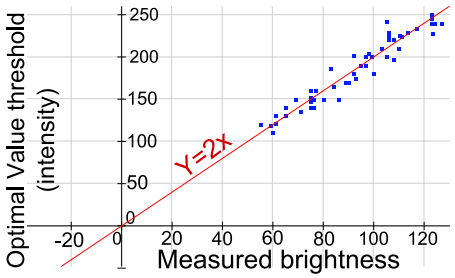

Figure 4: By comparing the optimal threshold value with the associated brightness value, we can see clearly that our 50 test images database (represented as blue squares in the image) follows the linear function $y = 2x$ (red line in the image), showing the proportionality between T_v and the global Brightness.

Thus, we computed the ratio $\frac{T_v}{Brightness}$ to estimate k_v.

$$T_v = \text{Brightness} * k_v. \quad (2)$$

The Saturation threshold T_s was set at a constant value because Saturation's behavior is depending on the color and brightness presenting difficulties to use in specularities detection. Our thresholding conditions is presented in Eq.(3).

$$\text{if } S(x) < T_s \text{ and } V(x) > T_v, \quad (3)$$

with $S(x)$ and $V(x)$ the Saturation and Value of the pixel x. Moreover, when oversaturation occurred, by watching the *saturated* value of the Value channel (with the value 255 in the histogram), we adjust automatically these thresholds following this formula (Eq.(4)):

$$\begin{gathered}\text{if } Histogram_{Value}(255) > (Image_{size}/3) \\ T_s = 30 \text{ and } T_v = 245.\end{gathered} \quad (4)$$

The thresholding step produces robust results under difficult conditions and allows a better control on the context. Indeed, we can disable the specularities detection if the image is oversaturated (high brightness) during lighting jumps to avoid false detections and provide reliability in a real-time application.

3.4 Post-processing

Even with our contrast equalization, some areas are still misdetected when the image is oversaturated (for example the piece of paper on the right as in Fig.5(a)).

We rely our post-processing on a new property of specularity reflections: gradient (see Fig.5(d)) which is represented in the HSV color space. The gradient discriminates effectively the specularity from a white region misdetected. In a first time, a division of the result image into k regions of specularity candidates is applied (Fig.5(b)). This segmentation is done using (Suzuki and Satoshi, 1985) algorithm. We took the biggest square for each contour because a specularity can have small fragments around it and it is more relevant to include them in the calculus. In a second time, by modifying the thresholds T_s and T_v, we will compute the area for each step to study its evolution. If this evolution is constant (decreases linearly over the time regularly (see Fig.6(a)) or the variation is null (see Fig.6(b)), this area is considered as a specular reflection. If the area decreases abruptly (see Fig.6(c) and Fig.6(d)), the area was misdetected as a specular reflection.

This criterion is common in every specularity but difficult to apply on very small surfaces because the gradient exists but is drastically smaller. Note that, in some cases, white areas could have a gradient aspect but this case remains rare.

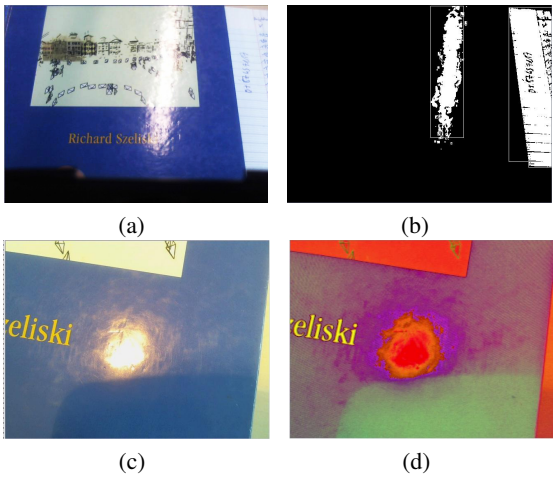

Figure 5: (a) Oversaturated image: the paper has an aspect very close to the specularity and could be misdetected as a specularity. (b) Isolation of the candidates for specularities of the figure (a). (c) Specularity seen in RGB color space. (d) Gradient property represented in the HSV color space. The gradient is clearly highlighted and discriminates the specularity from the white region in the top of the picture.

3.5 Algorithmic complexity

An algorithmic complexity study was conducted on every step of our method (see in Table.2). The global complexity computed is $O(n+k*c)$ with n representing the number of pixels in the image, k the number of regions found in our segmentation and c the number of iterations during our gradient process.

Table 2: Global complexity of our method. n represents all the pixels of the image. k is the number of regions found in our segmentation and c the number of iterations during the gradient thresholding.

Steps	Complexity
Contrast equalization	$O(1)$
Thresholding	$O(n)$
Segmentation + Gradient thresholding	$O(n*k)+O(k*c)$
Total:	$O(n+k*c)$

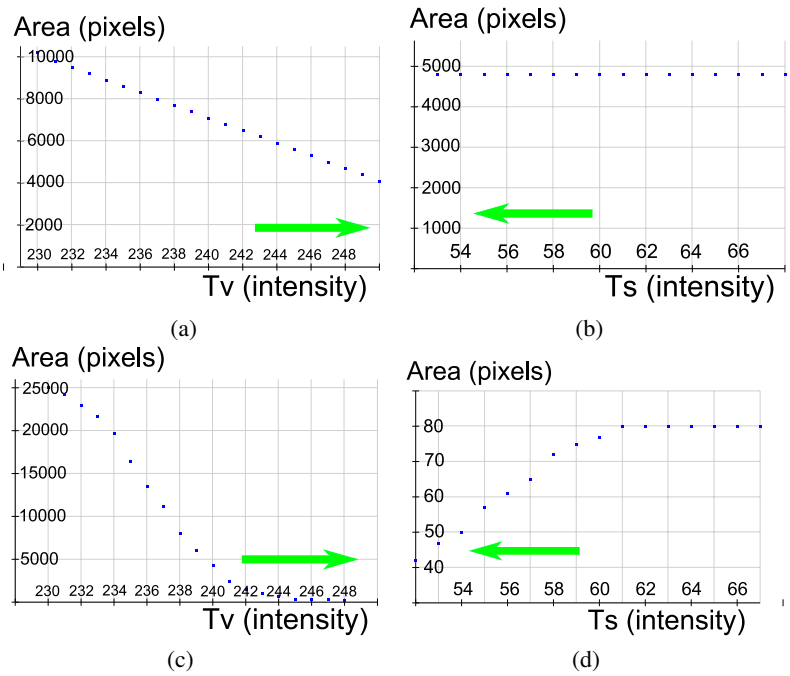

Figure 6: (a) and (b) represent the evolution of the specularity's area (in the middle of 5(b)). (c) and (d) represent the evolution of the white region's area (the book on the right of 5(b)). Area evolution is computed in function of T_v ((a) and (c)) and T_s ((b) and (d)). We can see clearly that the specularity has an area slowly decreasing and regularly when T_v is increasing and a constant area when T_s is decreasing. In contrast, the misdetected white has an area sharply decreasing when T_v is increasing. The same occurred when T_s is decreasing

4 EXPERIMENTAL EVALUATION

4.1 Experimental protocol

We compare our results with our implementation of Arnold et *al*. method which is a rapid state-of-the-art approach giving good results in real-time. Moreover, (Arnold et al., 2010) compared their method with (Oh et al., 2007) by pointing out efficiency and speed of their approach. The implementation of the method was done using (Arnold et al., 2010) parameters.

These approaches were tested on our database of 100 test images (different from our training database used to set the different thresholds) to highlight the genericity and efficiency of our method.

4.2 Quantitative evaluation

A reliable evaluation for specularities detection requires a clear definition of the specular reflections' properties. Two criteria should be highlighted: accuracy of the specularity's contour and exactness of the gravity center. The first criterion purposes to compare the contour of a specularity evaluated by the human eye with the output of our algorithm. Thus, a manual contouring of the specularities on our 100 test images database was done and compared with the contours of the specularities detected (gray scale images as seen in Fig.7). The contours are computed using Sobel operator with a 3×3 kernel. A contour is considered accurate if for each contour point, we find a pixel belonging in its neighborhood. This neighborhood is represented by a 9×9 matrix to be strict enough and not accept critical errors (Fig.8(a) demonstrates our *contour* evaluation).

In Fig.8(b), the principle of our *gravity center* evaluation is illustrated. By using our gradient supposition described in 3.4, a gravity center is found by following the opposite direction of the gradient until convergence (gradient stable or at the value of 255). The remaining points are used to compute a centroid more relevant than a centroid estimated with the specularity contour only. The ground truth was manually estimated as well. Both methods were evaluated on the same data including images from Arnold et *al*. article and our data base of 100 different images.

Our approach proves to be about 1.5 faster than Arnold et al.

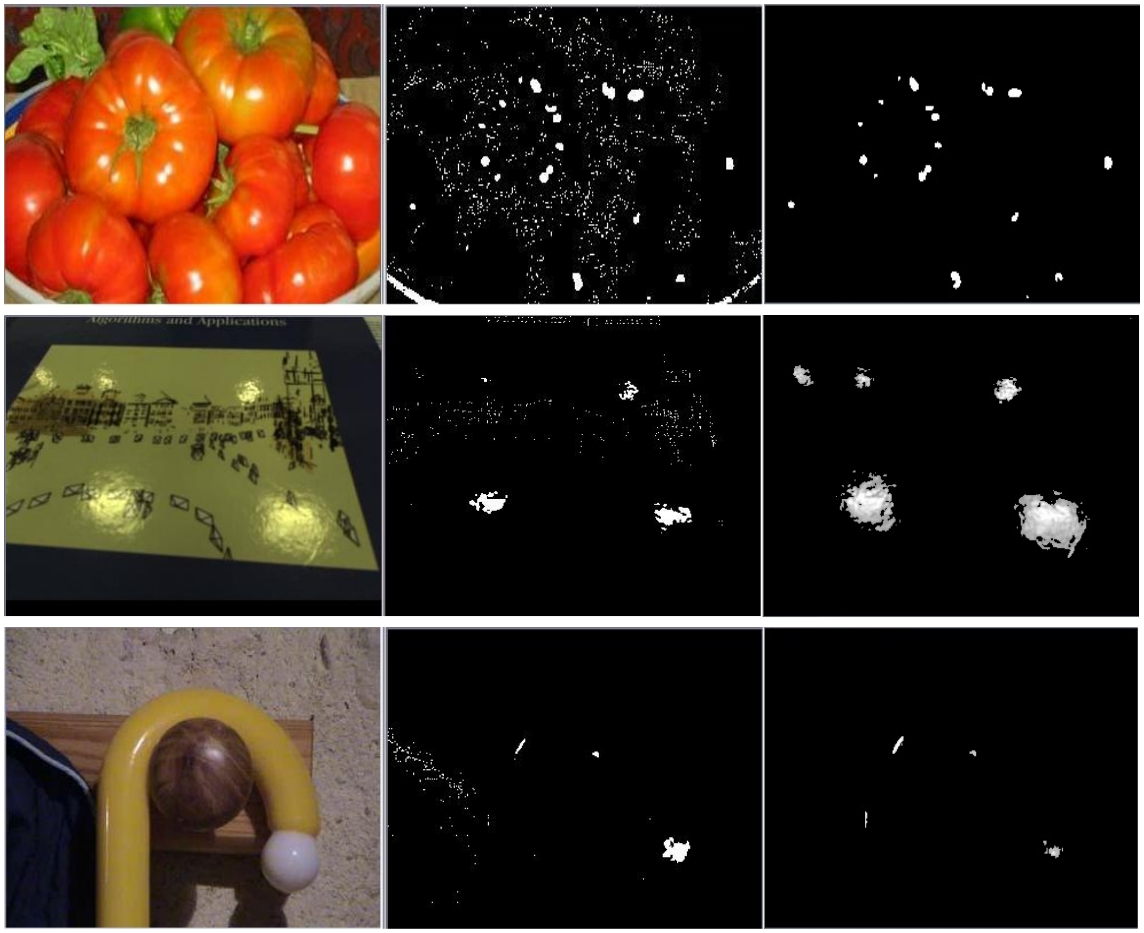

(a) Arnold et *al*. results in the middle: some noise is found and white is detected as a specularity. Our results, on the right, are clean and accurate

(b) Arnold et *al*. size criterion. The specularity detected was considered too big and was removed. Our gradient method successfully removed the unwanted white area.

Figure 7: Specular reflections detection results of Arnold et *al* method (in the middle) comparing with ours (on the right). These results were computed on our 100 test images database.

Table 3: Speed comparison between the two methods using the mean time of treatment on a single image on the database of 100 images.

Method / Evaluation	(Arnold et al., 2010)	**Our Method**
Elapsed time	0.0584 s	**0.0371 s**
Contour	70.3 %	**80.29 %**
Gravity center	67.2 %	**78.13 %**

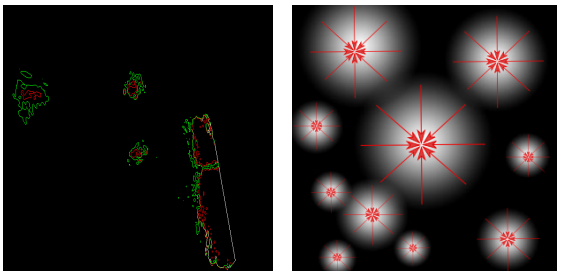

(a) (b)

Figure 8: Our proposed evaluation methods for specularity detection : *contour* and *gravity center* evaluation. (a) shows differences between the two methods using the ground truth (in green) and the current detection (in red). Common pixels are colored in gray. (b) illustrates the gravity center estimation. The red lines represent the direction vector of the gradient around the specularity

4.3 Qualitative evaluation

Compared to (Arnold et al., 2010), noise is greatly reduced for all images. Fig.7(b) highlights that a specularity can appear as a very large area. Using a size criterion as in (Arnold et al., 2010) is not relevant for a generic approach of specular reflections detection.

5 CONCLUSION

In this paper, we present a new approach for specularities detection in images, by using simple and efficient properties of specular reflections. We use the Value and Saturation channels in the HSV color space to estimate automatically different thresholds based on the global brightness of the image. Moreover, as a pre-processing step, we propose an automatic contrast adjustment to handle lighting jumps and also a gradient aspect of a specularity to manage the misdetected regions. Our method is then real-time, generic and reliable for different applications. This approach was compared with the state-of-the-art by using a new experimental protocol based on two properties: accuracy of the contour and the gravity center of a specular reflection.

6 DISCUSSION AND FUTURE WORK

State-of-the art approaches on specular reflections detection are threshold based methods. Nevertheless, relying on strong reflection models such as Lambertian model (Brelstaff and Blake, 1988) or separating diffuse and specular components (Tan et al., 2004) could be relevant to increase accuracy and noise reduction. Some applications such as (Jachnik et al., 2012) and (Lagger et al., 2008) for 3D pose estimation or refinement of the light sources or (Karsch et al., 2011) require a real-time specular reflections detector because they are dealing with video stream. Moreover, a video stream contains a huge amount of information to provide accurate misdetection correction such as white textures in an image to another (see example in (Lee and Bajcsy, 1992) or (Feris et al., 2006)). Our method could be further improved by using multi-view information and is fast enough to handle each frame in real-time.

REFERENCES

Arnold, M., Ghosh, A., Ameling, S., and Lacey, G. (2010). Automatic segmentation and inpainting of specular highlights for endoscopic imaging. *Journal on Image and Video Processing*, 2010:9.

Blake, A. and Brelstaff, G. (1988). Geometry from specularities. *International Conference on Computer Vision*, pages 394–403.

Brelstaff, G. and Blake, A. (1988). Detecting specular reflections using lambertian constraints. In *International Conference on Computer Vision*, ICCV.

Deng, Y., Manjunath, B., and Shin, H. (1999). Color image segmentation. In *Computer Vision and Pattern Recognition*, CVPR.

Feris, R., Raskar, R., Tan, K.-H., and Turk, M. (2006). Specular highlights detection and reduction with multi-flash photography. *Journal of the Brazilian Computer Society*, 12(1):35–42.

Jachnik, J., Newcombe, R. A., and Davison, A. J. (2012). Real-time surface light-field capture for augmentation of planar specular. In *International Symposium on Mixed and Augmented Reality*, ISMAR.

Karsch, K., Hedau, V., Forsyth, D., and Hoiem, D. (2011). Rendering synthetic objects into legacy photographs. *ACM Transactions on Graphics (TOG)*, 30(6):157.

Lagger, P., Salzmann, M., Lepetit, V., and Fua, P. (2008). 3d pose refinement from reflections. In *Computer Vision and Pattern Recognition*, CVPR.

Lambert, J. H. and DiLaura, D. L. (2001). *Photometry, or, on the measure and gradations of light, colors, and shade:translation from the Latin of photometria, sive, de mensura et gradibus luminis, colorum et umbrae*.

Lee, S.-T., Yoon, T.-H., Kim, K.-S., Kim, K.-D., and Park, W. (2010). Removal of specular reflections in tooth color image by perceptron neural nets. In *International Conference on Signal Processing Systems*, ICSPS.

Lee, S. W. and Bajcsy, R. (1992). Detection of specularity using color and multiple views. In *European Conference on Computer Vision*, ECCV.

Oh, J., Hwang, S., Lee, J., Tavanapong, W., Wong, J., and de Groen, P. C. (2007). Informative frame classification for endoscopy video. *Medical Image Analysis*, 11(2):110–127.

Ortiz, F. and Torres, F. (2005). A new inpainting method for highlights elimination by colour morphology. In *Pattern Recognition and Image Analysis*, pages 368–376.

Ortiz, F. and Torres, F. (2006). Automatic detection and elimination of specular reflectance in color images by means of ms diagram and vector connected filters. *Systems, Man, and Cybernetics, Part C: Applications and Reviews*, 36(5):681–687.

Park, J. B. and Kak, A. C. (2003). A truncated least squares approach to the detection of specular highlights in color images. In *International Conference on Robotics and Automation*, ICRA.

Saint-Pierre, C.-A., Boisvert, J., Grimard, G., and Cheriet, F. (2011). Detection and correction of specular reflections for automatic surgical tool segmentation in thoracoscopic images. *Machine Vision and Applications*, 22(1):171–180.

Shafer, S. A. (1985). Using color to separate reflection components. *Color Research & Application*, 10(4):210–218.

Sillion, F. and Puech, C. (1989). A general two-pass method integrating specular and diffuse reflection. In *Special Interest Group on GRAPHics and Interactive Techniques*, SIGGRAPH.

Stehle, T. (2006). Removal of specular reflections in endoscopic images. *Acta Polytechnica: Journal of Advanced Engineering*, 46(4):32–36.

Suzuki and Satoshi (1985). Topological structural analysis of digitized binary images by border following. *Computer Vision, Graphics, and Image Processing*, 30(1):32–46.

Tan, R. T., Nishino, K., and Ikeuchi, K. (2004). Separating reflection components based on chromaticity and noise analysis. *Pattern Analysis and Machine Intelligence*, 26(10):1373–1379.

Torres, F., Angulo, J., and Ortiz, F. (2003). Automatic detection of specular reflectance in colour images using the ms diagram. In *Computer Analysis of Images and Patterns*, CAIP.